https://doi.org/10.5194/egusphere-2026-2963
Preprint. Discussion started: 23 June 2026

Hydrological response regimes of compound hydroclimatic events across China revealed by behavior-space regionalization

LE Xinlong[1,2], KANG Ling[1,2,*], ZHOU Liwei[1,2]

[1]School of Civil and Hydraulic Engineering, Huazhong University of Science and Technology, Wuhan 430074 China.
[2]Joint International Water Security Research Center, Huazhong University of Science and Technology, Wuhan 430074 China.

Correspondence to: KANG Ling (kling@hust.edu.cn)

Abstract. Compound hydroclimatic events can trigger diverse hydrological responses, yet most large-scale assessments still characterize them primarily through event type, frequency, or intensity. Such event-centered descriptions may obscure the fact that the same compound anomaly can propagate through different hydrological pathways depending on antecedent conditions, soil-moisture storage, runoff response, seasonality, and regional hydroclimatic setting. Here we develop a behavior-space regionalization framework to diagnose hydrological response regimes of compound hydroclimatic events across China. Monthly standardized indices of thermal anomaly, meteorological moisture anomaly, soil moisture, and runoff are used to identify four compound-event types, including warm-wet, warm-dry, cold-wet, and cold-dry events. We then construct a multidimensional behavior-feature space that integrates event occurrence, conditional severity, persistence, seasonality, antecedent state, soil-moisture–runoff propagation, transition behavior, and threshold sensitivity. Based on this feature space, eight hydrological response regimes are identified and further grouped into three response pathways: amplification, propagation, and decoupling. The eight regimes show distinct behavior fingerprints, event-type coupling, antecedent-memory sensitivity, and spatial organization across major basins and climate zones. Seasonal high-intensity, soil-moisture propagation, and weak-response regimes account for the largest national fractions, but no single regime dominates China's compound-event response structure. Spatial transition analysis further reveals pronounced regime mixing along hydroclimatic transition belts, plateau-edge regions, and basin-climate boundaries. These findings show that compound hydroclimatic risk across China is organized by multiple hydrological response pathways rather than by a single gradient of event frequency or severity. The proposed framework provides a response-centered basis for regional hydroclimatic risk assessment and mechanism-specific monitoring.

1 Introduction

Compound hydroclimatic events have increasingly been recognized as critical drivers of regional climate and water-related risks because their impacts often emerge from the concurrence or sequential interaction of multiple climatic and hydrological anomalies rather than from a single variable alone (Hao et al., 2018; Leonard et al., 2014; Zscheischler et al., 2018, 2020). In contrast to conventional univariate extremes, compound events involve interactions among drivers, hazards, antecedent states, and response processes across different temporal and spatial scales. Such interactions may amplify agricultural stress, water-

https://doi.org/10.5194/egusphere-2026-2963
Preprint. Discussion started: 23 June 2026

resource insecurity, ecosystem degradation, flood risk, and drought impacts because thermal, meteorological, soil-moisture, and runoff anomalies can reinforce or offset one another(Liu et al., 2026; Tripathy et al., 2023; Wang et al., 2023). For example, warm-dry conditions may intensify atmospheric evaporative demand, accelerate soil-moisture depletion, and aggravate hydrological drought, whereas warm-wet or cold-wet conditions may modify runoff generation, seasonal storage, and delayed water availability(Liu et al., 2024a). Understanding how compound anomalies are translated into hydrological responses is therefore essential for improving regional hydroclimatic risk diagnosis and for moving beyond single-hazard assessment.

Previous studies have made substantial progress in defining compound events, developing statistical frameworks, and mapping their frequency, duration, intensity, spatial extent, and long-term trends (Hao et al., 2022; Zhang et al., 2021). Many hydroclimatic applications classify compound events according to combinations of thermal and moisture states, such as warm-dry, warm-wet, cold-dry, and cold-wet events (Manning et al., 2018; Ye et al., 2019). This event-type perspective is useful because it provides an intuitive way to describe the co-occurrence of temperature and moisture anomalies and to compare their spatial distributions under historical or future climate conditions. In China, such classifications have been widely used to examine compound drought and heatwave events, compound temperature–precipitation extremes, and the regional sensitivity of warm-dry and warm-wet risks under climate warming (Aihaiti et al., 2021; Pan et al., 2024) . These studies have substantially improved our understanding of where compound anomalies occur and how their occurrence characteristics have changed.

However, identifying the event type alone is insufficient for explaining how hydrological systems respond to compound hydroclimatic stress. The same warm-dry, warm-wet, cold-dry, or cold-wet event may lead to markedly different hydrological outcomes across regions because hydrological response depends not only on concurrent atmospheric anomalies but also on antecedent wetness, soil-moisture memory, catchment storage, runoff-generation mechanisms, snow or frozen-soil processes, vegetation condition, and seasonal timing (Seneviratne et al., 2010; Shukla and Wood, 2008; Van Loon, 2015; Vicente-Serrano et al., 2010). For instance, a warm-dry anomaly following a long wet antecedent period may produce a different soil-moisture and runoff response from the same anomaly occurring after persistent dryness(Gupta and Karthikeyan, 2024; Massari et al., 2023). Similarly, wet anomalies may generate rapid runoff amplification in humid or storage-saturated regions but only weak hydrological responses in arid regions where infiltration, evapotranspiration, and transmission losses dominate(Li et al., 2024; Massari et al., 2023; You et al., 2025). Therefore, an event-type map alone cannot reveal whether a region is characterized by rapid amplification, delayed propagation, persistent memory, weak coupling, or mixed transitions among hydroclimatic states(Li et al., 2026).

A key challenge is thus to move from compound-event identification toward response-regime diagnosis(Van Loon et al., 2024; Yang et al., 2025). Rather than asking only where a given compound-event type occurs, it is necessary to ask how compound events are organized into hydrologically meaningful response pathways(Ma et al., 2026; Niu et al., 2026). This requires a multidimensional behavior space that integrates event occurrence, conditional severity, persistence, seasonal timing, antecedent-state dependence, meteorological-to-soil-moisture propagation, soil-moisture-to-runoff propagation, and transition relationships among event types(Sutanto et al., 2025). Such a framework can help distinguish regions where hydroclimatic risk is mainly controlled by event intensity from regions where risk is governed by lagged land-surface memory, runoff

https://doi.org/10.5194/egusphere-2026-2963
Preprint. Discussion started: 23 June 2026

propagation, or weak and transitional coupling. This shift is particularly important for water-resource assessment because hydrological impacts are often produced by delayed or accumulated responses rather than by the instantaneous compound anomaly itself(Wang et al., 2025).

China provides an appropriate domain for developing such a framework because it spans strong gradients in moisture availability, temperature regime, topography, monsoon influence, snow and glacier effects, and river-basin characteristics (Niu et al., 2026). The humid monsoon regions of eastern and southern China, the arid and semiarid transition zones of northern and northwestern China, the Tibetan Plateau, and the complex mountain–basin systems in western China may exhibit fundamentally different pathways linking meteorological moisture anomalies to soil moisture and runoff. These geographic and climatic contrasts imply that compound hydroclimatic events are unlikely to follow a single national response pattern. Instead, major basins and climate zones may contain multiple response regimes, and the boundaries between regimes may form spatial transition belts where compound-event impacts are particularly difficult to interpret using conventional event-type classification.

In this study, we develop a behavior-space regionalization framework to diagnose hydrological response regimes of compound hydroclimatic events across China. Monthly standardized indices of thermal anomaly, meteorological moisture anomaly, soil moisture, and runoff are used to identify four compound-event types and to characterize their hydrological consequences. We then construct a multidimensional behavior-feature space and classify grid cells into hydrological response regimes. Specifically, this study addresses three questions: whether compound hydroclimatic events across China can be organized into distinct response regimes; how these regimes differ in behavior fingerprints, event-type coupling, antecedent-memory sensitivity, and propagation pathways; and how the resulting regimes are distributed across major basins, climate zones, and spatial transition belts. By shifting the focus from event-type mapping to response-regime diagnosis, this study provides a process-oriented basis for understanding compound hydroclimatic risk and its regional heterogeneity.

2 Study area and Research Data

2.1 Study area

China has diverse topography and climate conditions under the combined influence of the East Asian monsoon, the westerlies, and plateau thermal and dynamic processes. This setting produces strong regional contrasts in precipitation seasonality, evaporative demand, soil moisture storage, cryospheric conditions, and runoff generation. As a result, similar meteorological anomalies can trigger hydrological responses of different forms and magnitudes across regions, leading to pronounced spatial variability in compound hydrometeorological risks. Table 1 summarizes the study region using nine major river basins and seven climate zones.

Arid and semiarid regions in North China, Northwest China, and parts of Northeast China are generally more vulnerable to persistent warm dry compound events because of high evaporative demand and slow soil moisture recovery. By contrast, the humid monsoon influenced regions of the middle and lower Yangtze River, South China, and Southwest China are more likely

https://doi.org/10.5194/egusphere-2026-2963
Preprint. Discussion started: 23 June 2026

to experience warm wet and cold wet compound events. Over the Qinghai Tibet Plateau, complex terrain and high elevation further modify the interactions among temperature anomalies, freeze thaw processes, and runoff responses. These features make China an appropriate region for investigating the spatial heterogeneity of compound hydrometeorological risks. To improve regional interpretability, this study combines national gridded analysis with subregional assessments based on climate zones and major river basins. Climate zones are used to characterize differences in risk behavior under contrasting climatic regimes, while river basins are used to identify differences in propagation processes and antecedent memory within hydrological response units. This framework helps translate national scale results into region specific insights for adaptation and water resources management.

Table 1 Hydrological sub-basin and Climate zones

Hydrological divisions	Abbreviation	Climate zones	Abbreviation
Continental Basin	CB	Warm Temperate (Semi-humid)	WT-SH
Haihe River Basin	HaiRB	Mid-Temperate (Arid)	MT-A
Huaihe River Basin	HuaiRB	North Subtropical (Humid)	NST-H
Pearl River Basin	PRB	Mid-Temperate (Semi-humid)	MT-SH
Songhua and Liaohe River Basin	SLRB	Mid-Temperate (Semi-arid)	MT-SA
Southeast Basin	SEB	Plateau Temperate (Semi-arid)	PT-SA
Southwest Basin	SWB	Marginal Tropical (Humid)	MTr-H
Yangtze River Basin	YZRB	-	-
Yellow River Basin	YERB	-	-

2.2 Research Data

This study conducts a nationwide grid-based analysis using monthly-scale standardized indices. The four core variables employed represent temperature anomalies, meteorological drought, soil moisture anomalies, and runoff anomalies. Specifically, these include the standardized temperature index (STI), standardized precipitation-evapotranspiration index (SPEI), standardized soil moisture index (SSMI), and standardized runoff index (SRI). These four indices were constructed using a unified spatial grid and temporal range, and maintained spatiotemporal consistency throughout the study period to ensure consistency in the joint analysis of different variables.

https://doi.org/10.5194/egusphere-2026-2963
Preprint. Discussion started: 23 June 2026

During the data preprocessing stage, spatial and temporal coordinates for each variable were first standardized, with uniform naming conventions established for latitude, longitude, and time dimensions. Variables were rigorously aligned, retaining only those spatial and temporal samples where all four indices were present simultaneously. Subsequently, the temporal scale of the indices was filtered, and standardized time series on a unified temporal scale were selected for event identification and intensity analysis. Considering that nationwide-scale data may exhibit missing values and inconsistent sample sizes across different regions, this study further established a minimum valid month threshold to exclude grid samples with insufficient information, thereby ensuring the stability of subsequent joint distribution fitting, behavioral feature extraction, and clustering partitioning.

To support regional attribution analysis, this study also incorporates China's natural climatic zoning data and major river basin boundary data, converting all boundary data to a geographic coordinate system consistent with the index grid. Subsequently, through spatial overlay methods, the results of composite risk behavior partitioning at the grid cell level are aggregated to different climatic zones and river basin scales, thereby enabling an interpretive linkage between the national-level main results and regional contexts.

3 Materials and Methods

3.1 Overall Analytical Framework

This study establishes a grid-based analytical framework for diagnosing composite hydro-climatic risks on a national scale. This framework first identifies composite event types based on monthly-scale multivariate standardized indices, then quantifies the intensity of event conditions by integrating prior hydrometeorological background information. It further extracts behavioral characteristics of composite events in terms of frequency, persistence, intensity, seasonality, propagation relationships, and state transitions. Finally, it performs nationwide regional zoning based on behavioral similarity and conducts attribution analyses across different climatic zones and major river basins. Let the four types of standardized indices at grid point g and time t be denoted as:

$$X_{g,t}^{(1)} = \mathrm{STI}_{g,t},\ X_{g,t}^{(2)} = \mathrm{SPEI}_{g,t},$$

$$X_{g,t}^{(3)} = \mathrm{SSMI}_{g,t},\ X_{g,t}^{(4)} = \mathrm{SRI}_{g,t}$$

STI, SPEI, SSMI, and SRI represent the Standardized Temperature Index, Standardized Precipitation-Evapotranspiration Index, Standardized Soil Moisture Index, and Standardized Runoff Index, respectively. The analytical framework of this study comprises four main steps: dynamic identification of compound events; quantification of event intensity while accounting for time lags; extraction of behavioral characteristics of compound events; and regional partitioning and attribution analysis based on behavioral similarity.

https://doi.org/10.5194/egusphere-2026-2963
Preprint. Discussion started: 23 June 2026

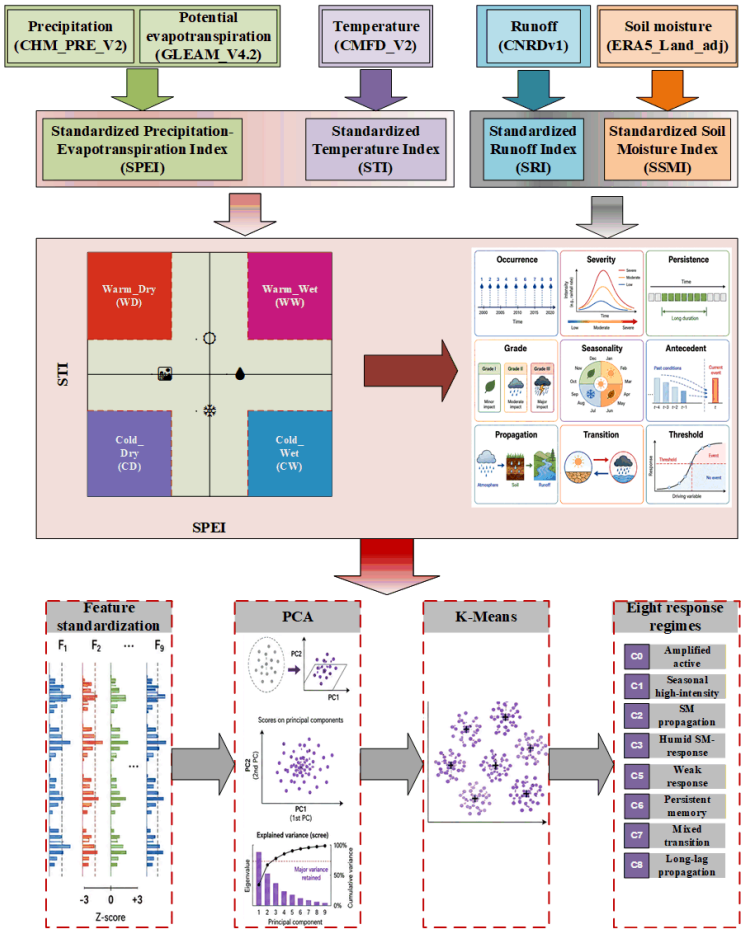

Figure 1. Workflow of the behavior-space regionalization framework for diagnosing hydrological response regimes of compound hydroclimatic events. The framework integrates standardized hydroclimatic indices, dynamic compound-event identification, lag-aware conditional intensity, multidimensional behavior-feature construction, clustering-based response-regime regionalization, regional attribution, and pathway-level hydrological interpretation.

3.2 Dynamic Identification of Compound Events

Traditional compound event studies typically use fixed thresholds for identification; however, for nationwide studies, this method struggles to adequately reflect background variations across different regions and months. To address this, this paper employs a dynamic threshold identification strategy based on grid cells and monthly empirical distributions. For each grid cell g and month m, the dynamic thresholds for high-temperature, low-temperature, wet, and dry conditions are defined as

$$\tau_{g,m}^{hot} = Q_{q_h}\left(STI_{g,t} \middle| month(t) = m\right)$$

$$\tau_{g,m}^{cold} = Q_{q_c}\left(STI_{g,t} \middle| month(t) = m\right)$$

$$\tau_{g,m}^{wet} = Q_{q_w}\left(STI_{g,t} \middle| month(t) = m\right)$$

https://doi.org/10.5194/egusphere-2026-2963
Preprint. Discussion started: 23 June 2026

$$\tau_{g,m}^{dry} = Q_{q_d}\left(STI_{g,t} \middle| month(t) = m\right)$$

Here, $Q_q(\cdot)$ denotes the empirical quantile function, while q_h, q_c, q_w, and q_d represent the quantile levels corresponding to high temperatures, low temperatures, humidity, and drought, respectively. In this way, thresholds can vary according to the month and regional context, thereby enhancing the consistency and comparability of risk identification across different regions at the national scale. Based on a combination of dynamic thresholds derived from temperature and aridity indices, this paper classifies composite events into four types: warm-wet, warm-dry, cold-wet, and cold-dry events. Let $E_{g,t}$ denote the event type at grid point g at time t, then

A warm-wet event is defined as $E_{g,t} = 1$, if $\mathrm{STI}_{g,t} \geq \tau_{g,m}^{hot}$ and $\mathrm{SPEI}_{g,t} \geq \tau_{g,m}^{wet}$

A warm-dry event is defined as $E_{g,t} = 2$, if $\mathrm{STI}_{g,t} \geq \tau_{g,m}^{hot}$ and $\mathrm{SPEI}_{g,t} \leq \tau_{g,m}^{dry}$

A cold-wet event is defined as $E_{g,t} = 3$, if $\mathrm{STI}_{g,t} \leq \tau_{g,m}^{cold}$ and $\mathrm{SPEI}_{g,t} \geq \tau_{g,m}^{wet}$

A cold-dry event is defined as $E_{g,t} = 4$, if $\mathrm{STI}_{g,t} \leq \tau_{g,m}^{cold}$ and $\mathrm{SPEI}_{g,t} \leq \tau_{g,m}^{dry}$

Specifically, for each grid cell and each calendar month, empirical distributions of temperature and moisture indices are constructed, and dynamic thresholds for high-temperature, low-temperature, humid, and dry conditions are determined based on these distributions. Subsequently, composite events are classified into four categories warm-wet events, warm-dry events, cold-wet events, and cold-dry events based on the combination of the signs of the temperature and moisture indices. When both temperature anomalies and dry-wet anomalies simultaneously meet the threshold conditions for the corresponding month, that month is classified as a compound event of the corresponding type; otherwise, it is recorded as a non-event state. Through this approach, event type identification no longer relies on a single fixed threshold but is better able to adapt to background variations across different regions and seasons. The advantage of this dynamic identification strategy is that it preserves the intuitiveness and interpretability of the four categories of composite event definitions while enhancing the comparability of results across different regions on a national scale. For areas with strong seasonality or markedly asymmetric background distributions, this approach helps reduce the systematic bias introduced by a uniform threshold.

3.3 Quantifying the Strength of Conditions for lagged Memorization

In compound event studies, event identification is not synonymous with event intensity. The fact that a given month is identified as a warm-dry or cold-wet event does not imply that its risk level can be measured solely by the absolute value of a single index. In fact, the severity of compound events is typically modulated by a combination of multi-process anomalies and prior background conditions. To address this, this paper, following event identification, further constructs a conditional intensity index that accounts for lagged memory to quantify the overall severity of different compound events.

In practice, we first apply empirical probability transformations to SPEI, STI, SRI, and SSMI, respectively, converting them into pseudo-observation sequences to mitigate the impact of differences in variable distributions on the joint analysis. Subsequently, we standardize the direction of the variables according to the type of compound event, ensuring that all variables

https://doi.org/10.5194/egusphere-2026-2963
Preprint. Discussion started: 23 June 2026

share a consistent meaning in the direction of increased event risk. For example, in the case of warm-dry events, increased high temperatures, worsening meteorological drought, expanding soil moisture deficits, and intensifying runoff deficits are all considered signals of heightened risk. After completing this directional alignment, this study utilizes joint dependency structures to estimate the conditional joint probability of the current event state given prior background conditions, and further maps this probability to a standardized conditional intensity index.

For any variable $X_{g,t}(j)$, its pseudo-observation is defined as

$$U_{g,t}^{(j)} = \widehat{F}_j\left(X_{g,t}^{(j)}\right), j = 1,2,3,4$$

Here, $\widehat{F}_j(.)$ denotes the empirical distribution function of the variable j. Considering the use of rank-based probability mapping in practical calculations, this paper further expresses the Gringorten plotting position as:

$$U_{g,t}^{(j)} = \frac{R_{g,t}^{(j)} - 0.44}{N_j + 0.12}$$

Here, $R_{g,t}^{(j)}$ denotes the sample rank, N_j represents the number of valid samples. Since the direction of risk amplification varies across different event types, it is necessary to standardize the direction. Let be the pseudo-observation of variable j for event type e after transformation in the direction of risk amplification, then

$$\widetilde{U}_{g,t}^{(j,e)} \begin{cases} U_{g,t}^{(j)}, + \\ 1 - U_{g,t}^{(j)}, - \end{cases}$$

For example, in the case of warm-dry events, the intensification of high temperatures, the worsening of meteorological drought, the expansion of soil moisture deficits, and the exacerbation of runoff deficits are all considered indicators of increased risk; therefore, the unified vector can be expressed as:

$$\widetilde{U}_{g,t}^{(j,e)} = \left(U_{g,t}^{(STI)}, 1 - U_{g,t}^{(SPEI)}, 1 - U_{g,t}^{(SRI)}, 1 - U_{g,t}^{(SSMI)}\right)$$

The severity of a compound event depends not only on the multivariate abnormal state at the current time but may also be jointly modulated by the preceding hydrometeorological background. To this end, this paper defines the risk state vector for event type e at the current time t as:

$$\boldsymbol{Z}_{g,t}^{(e)} = \left(\widetilde{U}_{g,t}^{(1,e)}, \widetilde{U}_{g,t}^{(2,e)}, \widetilde{U}_{g,t}^{(3,e)}, \widetilde{U}_{g,t}^{(4,e)}\right)$$

To explicitly account for the look-ahead memory effect, let the set of lag windows be:

$$L = l_1, l_2, l_3, \ldots\ldots, l_k$$

https://doi.org/10.5194/egusphere-2026-2963
Preprint. Discussion started: 23 June 2026

For example, $L = \{1\}$, $L = \{1, 2\}$, and $L = \{1, 2, 3\}$ represent antecedent windows that consider only the previous 1 month, the cumulative total of the previous 2 months, and the cumulative total of the previous 3 months, respectively. For a given window L, this paper defines the antecedent background aggregate of variable j under event type e as:

$$\overline{U}_{g,t}^{(j,e,L)} = \sum_{l \in L} w_l \widetilde{U}_{g,t-l}^{(j,e)}, \sum_{l \in L} w_l = 1$$

Here, wl is the forward lag weight. Consequently, the previous period's background vector is defined as:

$$\overline{\boldsymbol{A}}_{g,t}^{(e,L)} = \left(\overline{U}_{g,t}^{(1,e,L)}, \overline{U}_{g,t}^{(2,e,L)}, \overline{U}_{g,t}^{(3,e,L)}, \overline{U}_{g,t}^{(4,e,L)}\right)$$

Based on the current risk state and prior background vector described above, this paper defines the joint risk of a compound event under given prior background conditions as the conditional joint probability, that is:

$$p_{g,t}^{(e,L)} = C_e\left(Z_{g,t}^{(e)} \,\middle|\, \overline{A}_{g,t}^{(e,L)}\right)$$

Here, $C_e(\cdot)$ denotes the conditional joint probability function for event type e. It represents the joint probability that the current multivariate risk state simultaneously reaches a given level, given a known hydroclimatic background. Furthermore, the above conditional joint probability can be written as:

$$p_{g,t}^{(e,L)} = Pr\left(U_1 \le \widetilde{U}_{g,t}^{(1,e)}, U_2 \le \widetilde{U}_{g,t}^{(2,e)}, U_3 \le \widetilde{U}_{g,t}^{(3,e)}, U_4 \le \widetilde{U}_{g,t}^{(4,e)} \middle| \overline{\boldsymbol{A}}_{g,t}^{(e,L)}\right)$$

To enhance the comparability of results across different regions, event types, and lag windows, this paper further maps the conditional joint probability to the standard normal space and defines the conditional intensity index accounting for lags as:

$$CI_{g,t}^{(e,L)} = \Phi^{-1}\left(p_{g,t}^{(e,L)}\right)$$

Here,Φ^{-1}denotes the inverse function of the standard normal distribution; the larger the value of $CI_{g,t}^{(e,L)}$, the higher the joint risk of the composite event under the given antecedent background conditions. Compared to definitions that rely solely on the intensity of the current anomaly state, this conditional intensity index explicitly captures the influence of antecedent memory on the estimation of composite event severity, and thus serves as the core formula in the methodological framework of this paper.

To examine the effect of different lengths of antecedent memory on estimates of conditioning strength, this paper further defines the strength increment between different antecedent windows as:

$$\Delta CI_{g,t}^{(e;L_a \to L_b)} = CI_{g,t}^{(e,L_b)} - CI_{g,t}^{(e,L_a)}$$

Here, L_a and $L_b$denote two different settings for the early−memory window. If $\Delta CI_{g,t}^{(e;L_a \to L_b)} > 0$, this indicates that the event-conditional intensity increases as the early-memory window is expanded; conversely, it indicates that the conditional intensity

https://doi.org/10.5194/egusphere-2026-2963
Preprint. Discussion started: 23 June 2026

decreases after expanding the early-memory window. At the regional scale, this paper further defines the average lag sensitivity of an event type e as:

$$\overline{\Delta CI}^{(e;L_a\to L_b)} = \frac{1}{N_e}\sum_{g,t:E_{g,t}=e}\left[CI_{g,t}^{(e,L_b)} - CI_{g,t}^{(e,L_a)}\right]$$

Here, N_e represents the total number of samples for event type e. This formula is used to assess the overall sensitivity of the antecedent window to conditional intensity at the national scale, as well as across different climatic regions and river basins. This metric directly addresses a key scientific question in this study: whether different regions and event types exhibit consistent responses to the length of the antecedent hydrometeorological memory. To further distinguish between general events and high-intensity events, let the threshold for the conditional intensity level be

$$G_{g,t}^{(e,L)} = \begin{cases} 1, & CI_{g,t}^{(e,L)} < \gamma_1 \\ 2, \gamma_1 \le CI_{g,t}^{(e,L)} < \gamma_2 \\ 3, \gamma_2 \le CI_{g,t}^{(e,L)} < \gamma_3 \\ 4, & CI_{g,t}^{(e,L)} \ge \gamma_3 \end{cases}$$

3.4 Extraction of Behavioral Characteristics in Compound Events

To identify regions with similar risk behaviors on a national scale, this paper does not directly cluster the raw index sequences; instead, it first encodes the evolution of compound events at each grid cell into a set of multidimensional behavioral features. These features describe the organizational patterns of compound risks in different regions from multiple perspectives. Let the annual average frequency of event type e at grid point g be

$$F_g^{(e)} = \frac{1}{Y}1\left(E_{g,t} = e\right)$$

Here, Y represents the number of years in the study period, and 1(.) denotes the indicator function. The average duration of the event is defined as

$$D_g^{(e)} = \frac{1}{n_e}\sum_{r=1}^{n_e} d_r^{(e)}$$

Here, $d_r^{(e)}$ denotes the duration of the rth consecutive event, and n_e denotes the number of events. The average event intensity is defined as

$$\bar{C}I_g^{(e,L)} = \frac{1}{n_e}\sum_{t:E_{g,t}=e} C\,I_{g,t}^{(e,L)}$$

https://doi.org/10.5194/egusphere-2026-2963
Preprint. Discussion started: 23 June 2026

The maximum intensity is defined as

$$CI_{g,max}^{(e,L)} = \max_{t:E_{g,t}=e} C\,I_{g,t}^{(e,L)}$$

To characterize the propagation relationships among composite events, this paper also defines the propagation correlation coefficient between variable *i* and variable *j* with a lag of *l* as

$$\rho_g^{(i,j)}(l) = Corr\left(X_{g,t}^{(i)}, X_{g,t+l}^{(j)}\right)$$

This equation is used to describe the propagation characteristics of meteorological anomalies to soil moisture anomalies, and of soil moisture anomalies to runoff anomalies. Furthermore, to reflect the state transition relationships between event types, this paper further calculates the event transition probabilities.

$$P_{ab,g} = Pr\left(E_{g,t+1} = b \middle| E_{g,t} = a\right)$$

Here, a and b represent different event types and non-event states. Taking into account the aforementioned frequency, persistence, intensity, propagation relationships, state transitions, and prior background characteristics, the composite event behavior vector for grid point g is denoted as

$$\boldsymbol{f}_g = \left(F_g^{(1)}, \ldots, F_g^{(4)}, D_g^{(1)}, \ldots, D_g^{(4)}, \overline{CI}_g^{(1,L)}, \ldots, \overline{CI}_g^{(4,L)}, P_{ab,g}, \rho_g^{(i,j)}(l), \ldots\right)$$

Through the above processing, each grid cell no longer corresponds solely to a time series but is represented as a multidimensional compound event behavior vector. This vector comprehensively reflects the frequency, duration, intensity, seasonal patterns, prior context, and propagation relationships of the compound risks in that area, providing a foundation for subsequent behavioral zoning.

3.5 Dividing regions according to similarities in behavior

After obtaining the grid-level behavioral characteristics, this paper first standardizes all features and excludes grid samples with insufficient valid months or too few event samples to ensure the robustness of the cluster analysis. Assuming there are N valid grids nationwide, a feature matrix can be constructed

$$\boldsymbol{F} = [\boldsymbol{f}_1, \boldsymbol{f}_2, \ldots, \boldsymbol{f}_N]^{\mathrm{T}}$$

To reduce redundancy among high-dimensional behavioral features and extract a more compact behavioral representation, this paper applies an embedding transformation to $\boldsymbol{F}$ to obtain the low-dimensional representation $\boldsymbol{z_g}$. Clustering analysis is then performed in the low-dimensional space. Let the number of clusters be K, and the center of the kth cluster be μ_k. Then, the cluster category of grid point g is defined as

$$c_g = \arg\min_{k\in\{1,\ldots,K\}} |\boldsymbol{z_g} - \mu_k|^2$$

https://doi.org/10.5194/egusphere-2026-2963
Preprint. Discussion started: 23 June 2026

In this model, the national grid is divided into several regional units with similar compound event behavior characteristics. To avoid the number of clusters being entirely dependent on subjective settings, this paper further evaluates different candidate numbers of clusters using metrics such as the slenderness ratio, inter-cluster separation, intra-cluster compactness, cluster stability, and cluster size balance, and selects the optimal solution based on these criteria, ensuring both statistical validity and spatial interpretability. It should be noted that the classifications presented in this paper are not traditional geographical or climatic classifications, but rather functional classifications based on the behavioral characteristics of compound events; as such, they better reflect the differences among various regions across the country in terms of risk frequency, persistence, prior memory, and transmission chains.

3.6 Regional Attribution Analysis at the Climate Zone and Basin Scales

To further elucidate the regional significance of the national behavioral zoning results, this study spatially overlays the grid-scale compound risk behavioral zoning with the boundaries of China's natural climatic regions and major river basins. On the one hand, at the climatic region scale, we calculate the composition ratios of different clusters within each region, as well as the frequency and average intensity of various composite events and their sensitivity to prior conditions, to reveal how different climatic backgrounds influence composite risk behavior. On the other hand, at the river basin scale, we focus on comparing the dominant types of composite events, propagation lag relationships, the proportion of long-duration events, and the share of high-intensity events across different river basins to reflect differences in risk organization across distinct hydrological response units.

In addition, based on the results of conditional intensity under different antecedent windows, this study further calculates the regional average magnitude of change to assess the sensitivity of different climate zones and river basins to the length of lead-time memory. Through this analytical approach, which combines national-level results with regional-scale attribution, this study not only identifies the overall patterns of compound hydrometeorological risks in China but also elucidates the mechanisms underlying the formation and manifestation of these patterns in different climate and river basin contexts.

4 Results

4.1 Behavior-space differentiation of hydrological response regimes

The behavior-feature space revealed a structured organization of compound hydroclimatic responses across China. The behavior-space projection showed that the eight clusters occupied partially separated regions, indicating that the response regimes were not produced by a single frequency or severity gradient. Instead, the clusters reflected different combinations of event occurrence, conditional intensity, persistence, seasonality, antecedent memory, propagation coupling, and transition behavior. The centroid fingerprints further demonstrated that each regime was associated with a distinct feature signature (Figure 2).

https://doi.org/10.5194/egusphere-2026-2963
Preprint. Discussion started: 23 June 2026

The evidence-based naming analysis showed that the eight regimes had clear hydrological interpretations (Figure 3). C0 was identified as an amplified active regime because it showed strong conditional amplification and active dominant-event behavior. C1 was classified as a seasonal high-intensity regime, with high conditional intensity concentrated in specific seasonal windows. C2 was named soil-moisture propagation because its discriminative features were dominated by lagged SPEI–SSMI and SSMI–SRI dependencies. C3 represented a humid soil-moisture response regime, indicating antecedent soil-moisture control under humid hydroclimatic settings. C4 was interpreted as a weak-response regime because of weak soil-moisture–runoff coupling and limited hydrological amplification. C5 was identified as persistent memory, characterized by long event duration and stronger same-type transition behavior. C6 represented a mixed-transition regime with stronger warm-wet and cold-dry contributions and more mixed event transitions. C7 was interpreted as long-lag propagation, reflecting longer-lag transfer from meteorological moisture anomalies to soil moisture and runoff.

The similarity and hierarchy analysis further confirmed that the eight regimes were not isolated classes but formed a structured response hierarchy (Figure 4). The pairwise distance matrix and hierarchical clustering showed that some regimes were closely related, whereas others represented more distinct response modes. C0 and C1 were closely connected within an amplification-oriented branch. C2, C4, C3, and C7 occupied an intermediate space associated with propagation and response modulation. C5 and C6 showed relatively distinct positions, suggesting that persistent-memory and mixed-transition behavior represent specialized response modes rather than simple variants of the dominant event-frequency pattern. At the pathway level, the amplification pathway showed stronger severity and seasonality signals, the propagation pathway was characterized by persistence, antecedent-state, and propagation-related behavior, and the decoupling pathway was associated with weaker severity but stronger transition and boundary-related behavior. Together, Figures 2, 3, and 10 demonstrate that the clustering result is not a purely statistical partition. It represents a hydrologically interpretable hierarchy of compound-event response behavior.

https://doi.org/10.5194/egusphere-2026-2963
Preprint. Discussion started: 23 June 2026

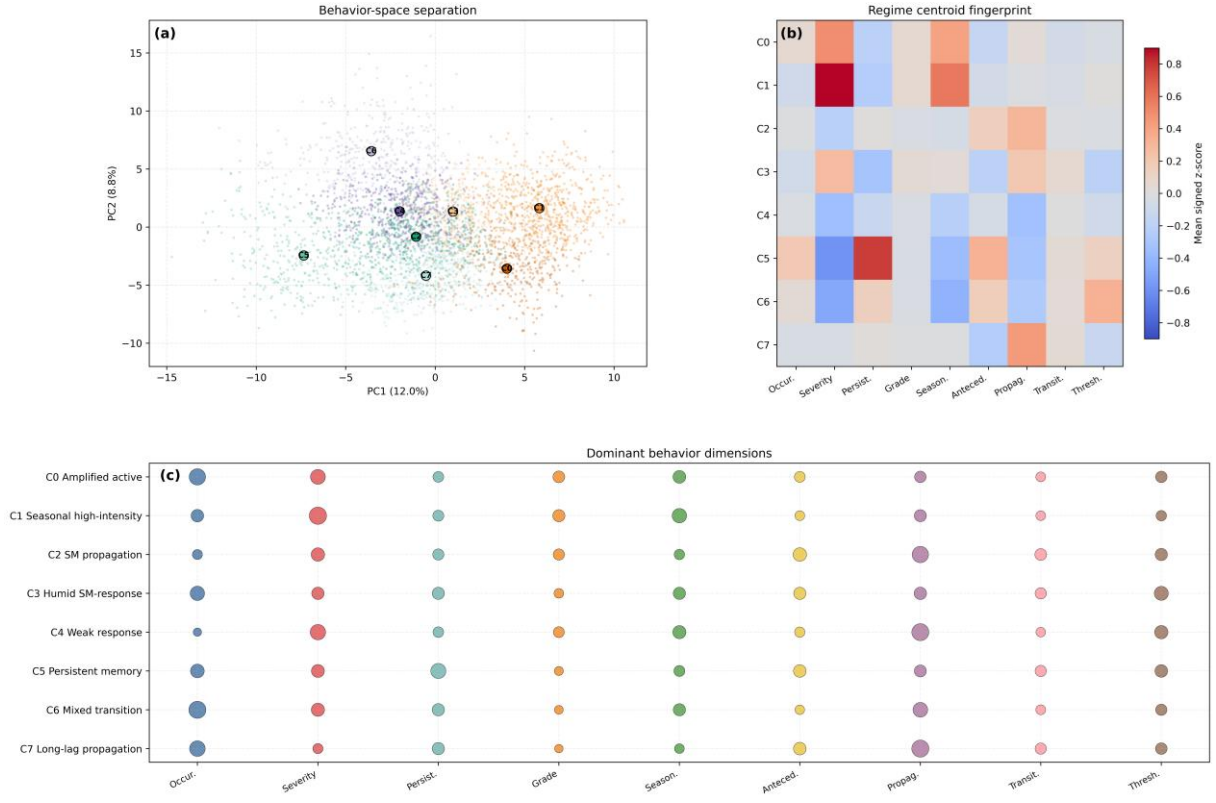

Figure 2. Behavior-space separation and regime fingerprints of the eight hydrological response regimes. Panel (a) shows the distribution of grid cells in the reduced behavior space. Panel (b) presents the signed centroid fingerprint of each regime across major behavior dimensions. Panel (c) shows the dominant behavior dimensions that contribute to regime differentiation.

https://doi.org/10.5194/egusphere-2026-2963
Preprint. Discussion started: 23 June 2026

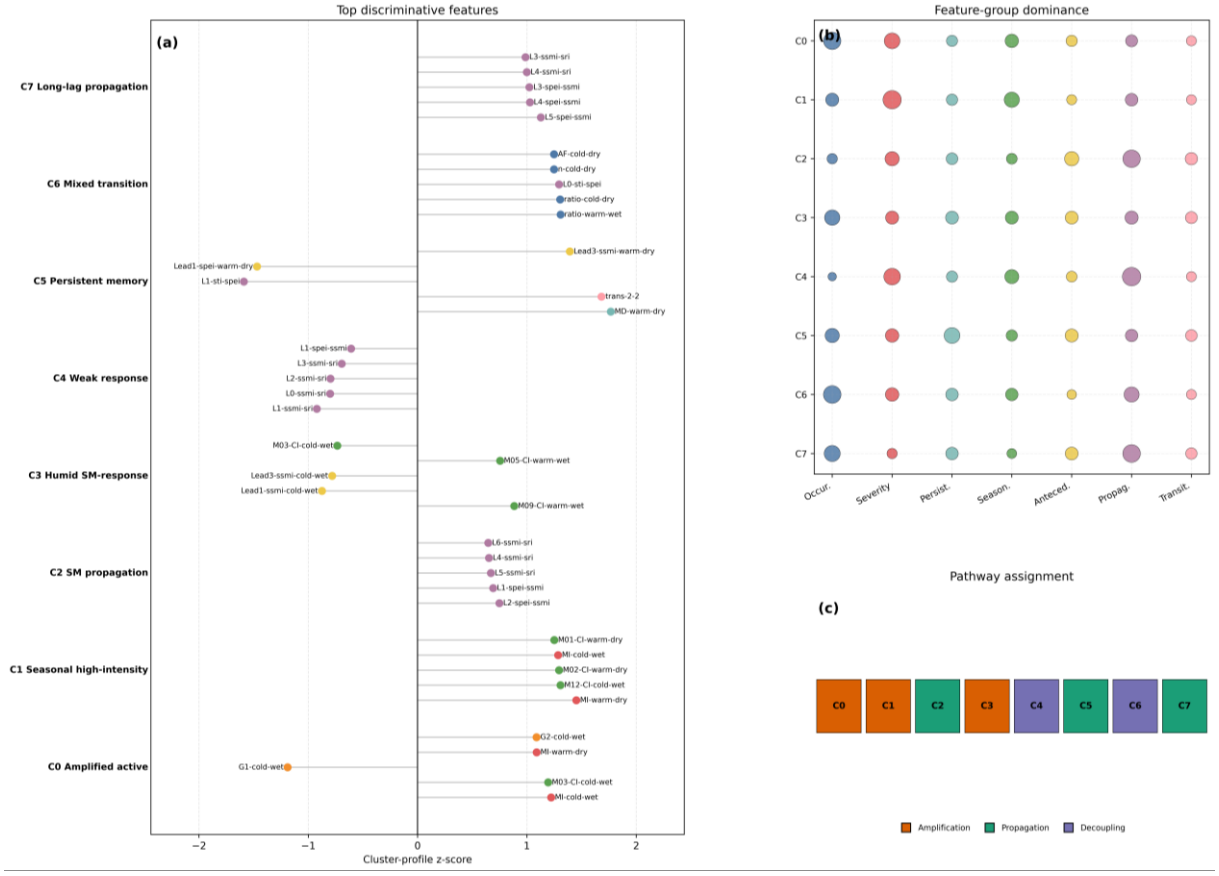

Figure 3. Evidence-based naming of the eight hydrological response regimes. Panel (a) shows the top discriminative features for each regime. Panel (b) summarizes feature-group dominance. Panel (c) assigns the eight regimes to three broader hydrological response pathways: amplification, propagation, and decoupling.

https://doi.org/10.5194/egusphere-2026-2963
Preprint. Discussion started: 23 June 2026

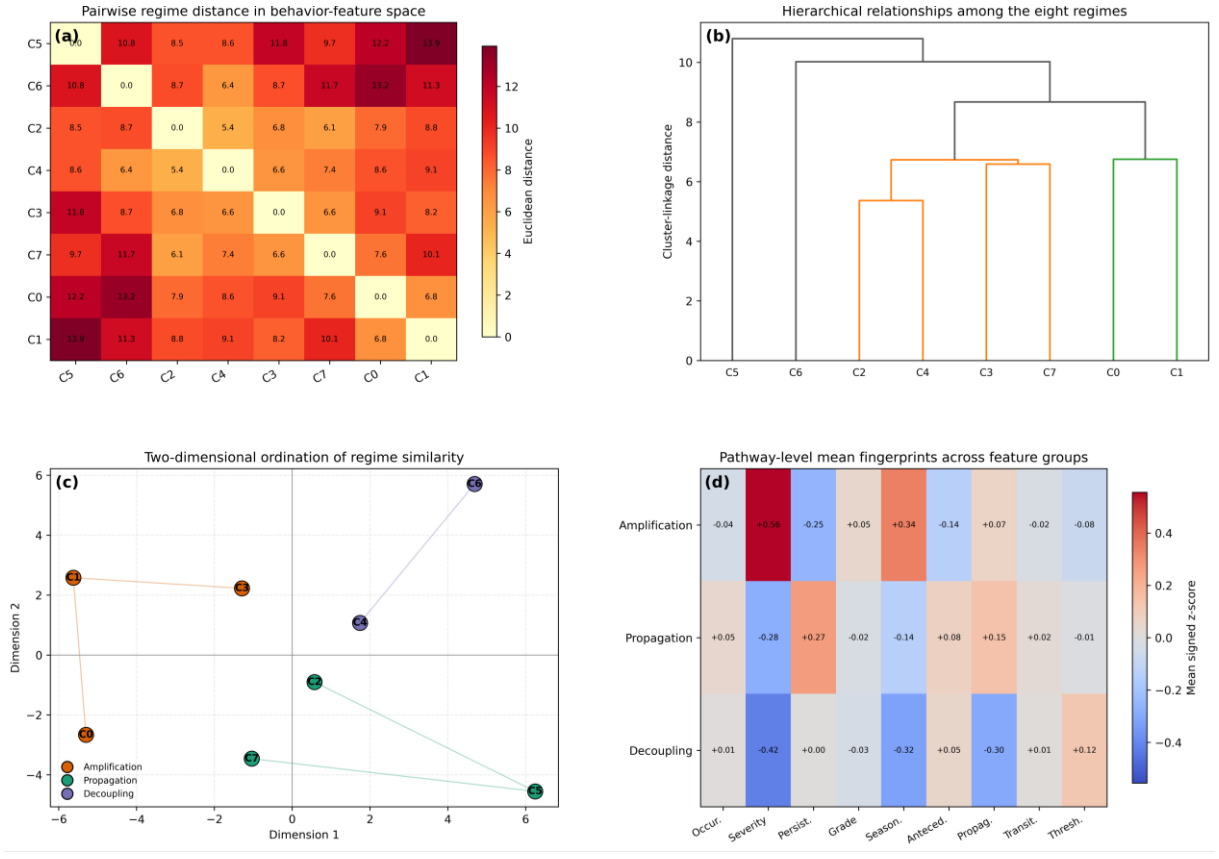

Figure 4. Similarity, hierarchy, and pathway structure of the eight response regimes. Panel (a) shows pairwise distances among regimes in the behavior-feature space. Panel (b) presents hierarchical clustering relationships. Panel (c) shows a two-dimensional ordination of regime similarity. Panel (d) summarizes pathway-level mean fingerprints across feature groups.

4.2 Added hydrological value of the eight-regime solution

The comparison between the four-class and eight-regime solutions showed that the refined k = 8 regionalization provided additional hydrological information beyond a coarse national classification (Figure 5). The cluster-number diagnostics indicated that k = 4 offered a parsimonious broad partition, but the alluvial transition from k = 4 to k = 8 revealed that each coarse class was split into multiple refined regimes. This shows that the four-class solution mainly captured broad hydroclimatic contrasts, whereas the eight-regime solution separated different hydrological response pathways hidden within the same coarse class.

The transition matrix further demonstrated that the relationship between k = 4 and k = 8 was not one-to-one. Some k = 4 classes were divided into amplification-related regimes, while others split into propagation, memory, weak-response, or transition regimes. This refinement is hydrologically important because similar broad climatic classes can contain different soil-moisture–runoff coupling structures, seasonal response behaviors, and antecedent-memory effects.

https://doi.org/10.5194/egusphere-2026-2963
Preprint. Discussion started: 23 June 2026

The basin heterogeneity analysis also showed that k = 8 increased within-basin differentiation relative to k = 4. This result indicates that major river basins are not internally homogeneous response units. Large basins can simultaneously contain amplification-dominated areas, propagation zones, and weak or transitional response regions. Thus, the eight-regime solution provides a more suitable resolution for diagnosing hydrological response behavior than the coarser four-class partition. The k = 8 solution was therefore selected not merely as a statistical option, but as a hydrologically meaningful scale that balances interpretability, regional differentiation, and response-pathway separation.

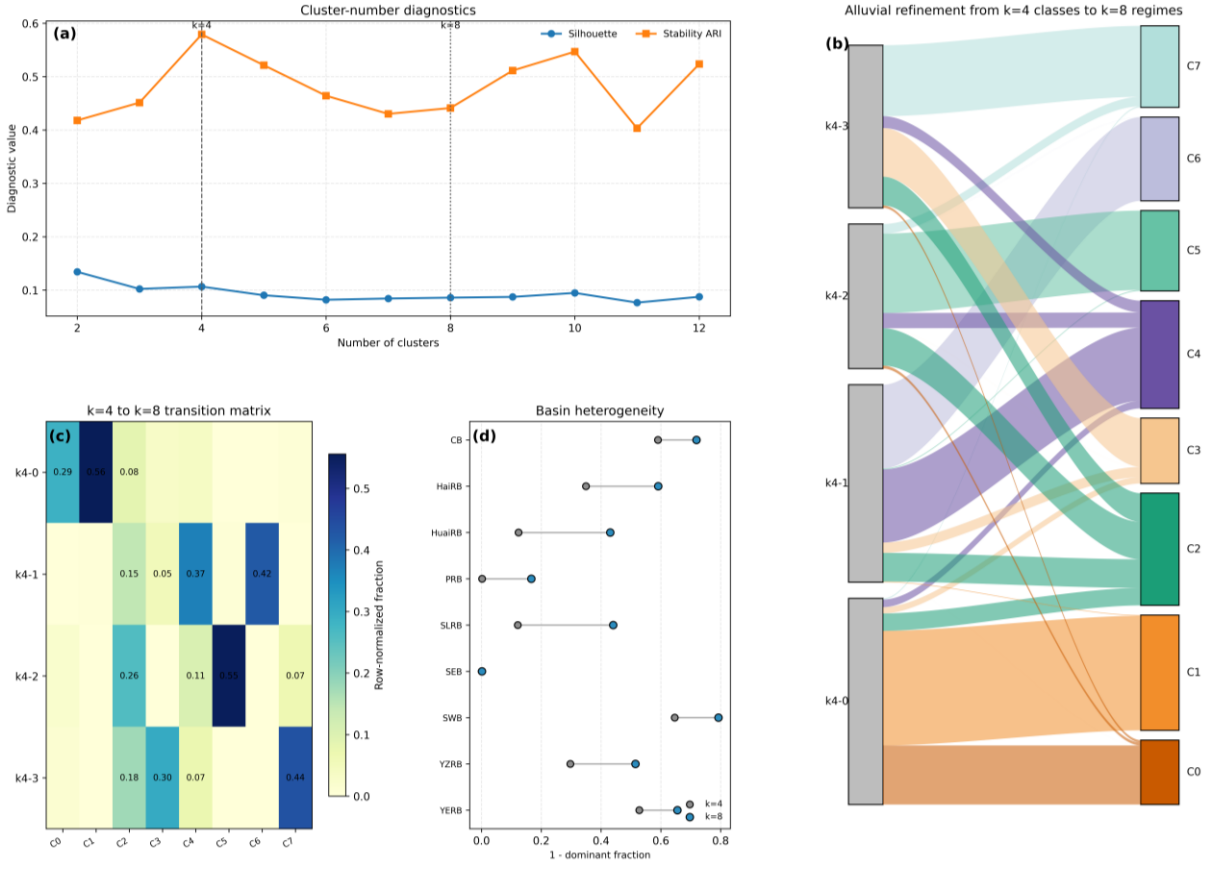

Figure 5. Added hydrological information from the eight-regime solution relative to the four-class solution. Panel (a) presents cluster-number diagnostics. Panel (b) shows the alluvial refinement from k = 4 coarse classes to k = 8 regimes. Panel (c) gives the k = 4 to k = 8 transition matrix. Panel (d) compares basin heterogeneity under the two classification levels.

4.3 Spatial organization, regional attribution, and transition belts

The eight response regimes showed strong spatial organization across China (Figure 6). The seasonal high-intensity regime C1 occupied the largest national area fraction, accounting for approximately 16.2% of the valid area. It was followed by C2 soil-moisture propagation at 15.8% and C4 weak response at 15.2%. The remaining regimes each contributed approximately

https://doi.org/10.5194/egusphere-2026-2963
Preprint. Discussion started: 23 June 2026

9–12% of the national valid area, indicating that China's compound-event response structure is not dominated by a single regime. Instead, multiple response modes coexist at comparable spatial scales.

The spatial pattern showed clear pathway-level contrasts. Amplification-related regimes were mainly distributed in southern and southeastern China, where compound events are more likely to trigger strong seasonal or conditional responses. Propagation regimes were more evident in northern, western, and transitional regions, where soil-moisture storage and runoff response mediate the effect of meteorological anomalies. Weak and mixed-transition regimes appeared in areas with complex topography, arid background conditions, or weaker soil-moisture–runoff coupling.

Regional attribution further highlighted that major basins and climate zones contain distinct mixtures of response regimes (Figure 7). The Southeast Basin and Pearl River Basin were strongly dominated by C1, indicating seasonal high-intensity amplification. The Southwest Basin was characterized by C0, suggesting amplified active response behavior. The Haihe and Yellow River basins showed stronger representation of C2, consistent with a propagation-oriented response pathway. The Continental Basin was dominated by C4, reflecting weak hydrological amplification under arid or internally drained conditions. At the climate-zone scale, humid and subtropical regions tended to be associated with amplification regimes, whereas semiarid and plateau-related zones showed stronger propagation or weak-transition behavior.

The ternary pathway attribution confirmed that regional differences were better interpreted through three response pathways than through individual regimes alone. Several southern and humid regions were located near the amplification vertex, whereas northern and transitional regions shifted toward the propagation side. The regime-richness analysis showed that the Southwest Basin, Yellow River Basin, Continental Basin, and several semiarid or plateau climate zones contained a larger effective number of regimes. This suggests stronger internal heterogeneity and more complex response mixtures in these regions.

The spatial transition analysis further revealed that regime boundaries were not randomly distributed (Figure 8). High local transition intensity and regime richness appeared along major hydroclimatic transition belts, including northwestern semiarid margins, plateau-edge regions, and zones separating humid southern regimes from northern propagation-dominated regimes. The most frequent adjacent regime boundary was C4–C6, accounting for approximately 14.5% of all regime boundaries, followed by C2–C4 at 11.0%, C0–C1 at 9.2%, and C2–C7 at 8.7%. These boundary types indicate that the most active spatial transitions occurred between weak-transition, propagation-memory, and amplification-related regimes. Therefore, the response-regime map should not be interpreted only as a distribution of dominant classes. It also reveals regime cores, transition belts, and mixing hotspots that reflect the spatial organization of hydrological response mechanisms.

https://doi.org/10.5194/egusphere-2026-2963
Preprint. Discussion started: 23 June 2026

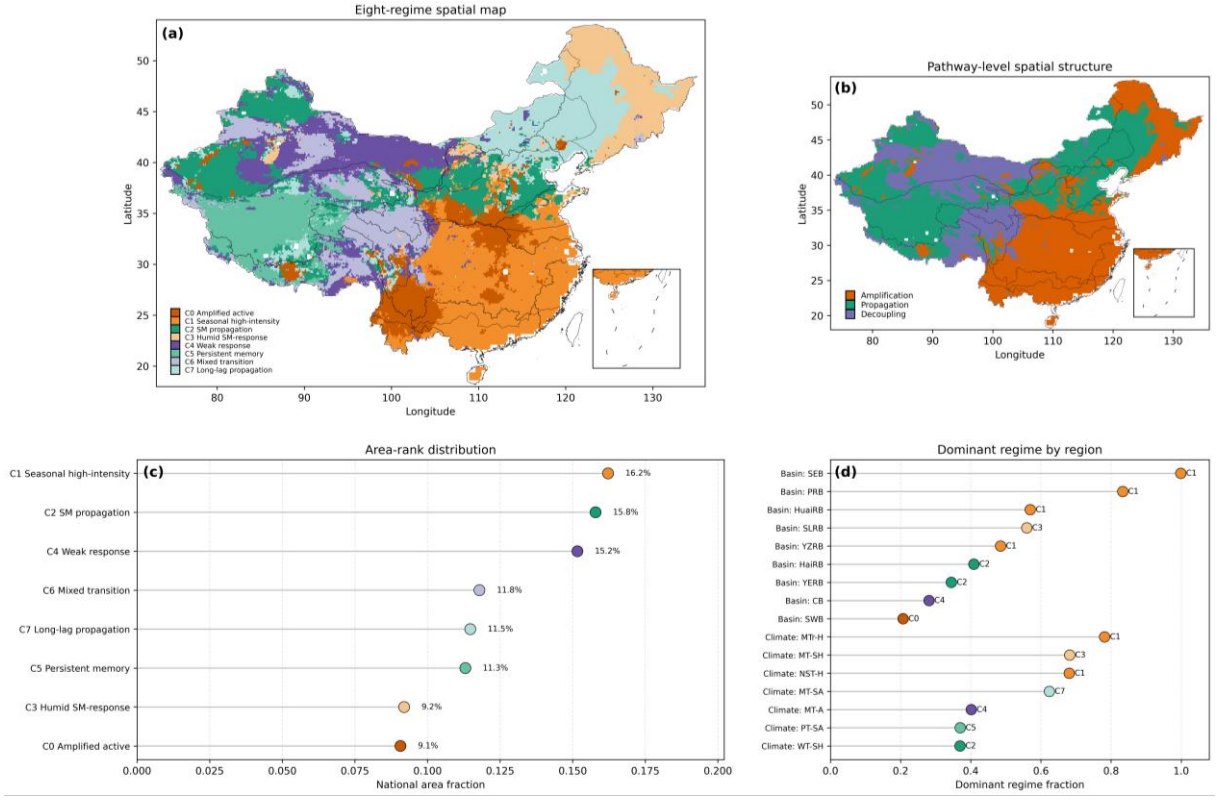

Figure 6. Spatial organization of the eight hydrological response regimes across China. Panel (a) maps the eight response regimes. Panel (b) shows their aggregation into three pathway-level spatial structures. Panel (c) presents the national area fraction of each regime. Panel (d) identifies the dominant regime in each major basin and climate zone.

https://doi.org/10.5194/egusphere-2026-2963
Preprint. Discussion started: 23 June 2026

405

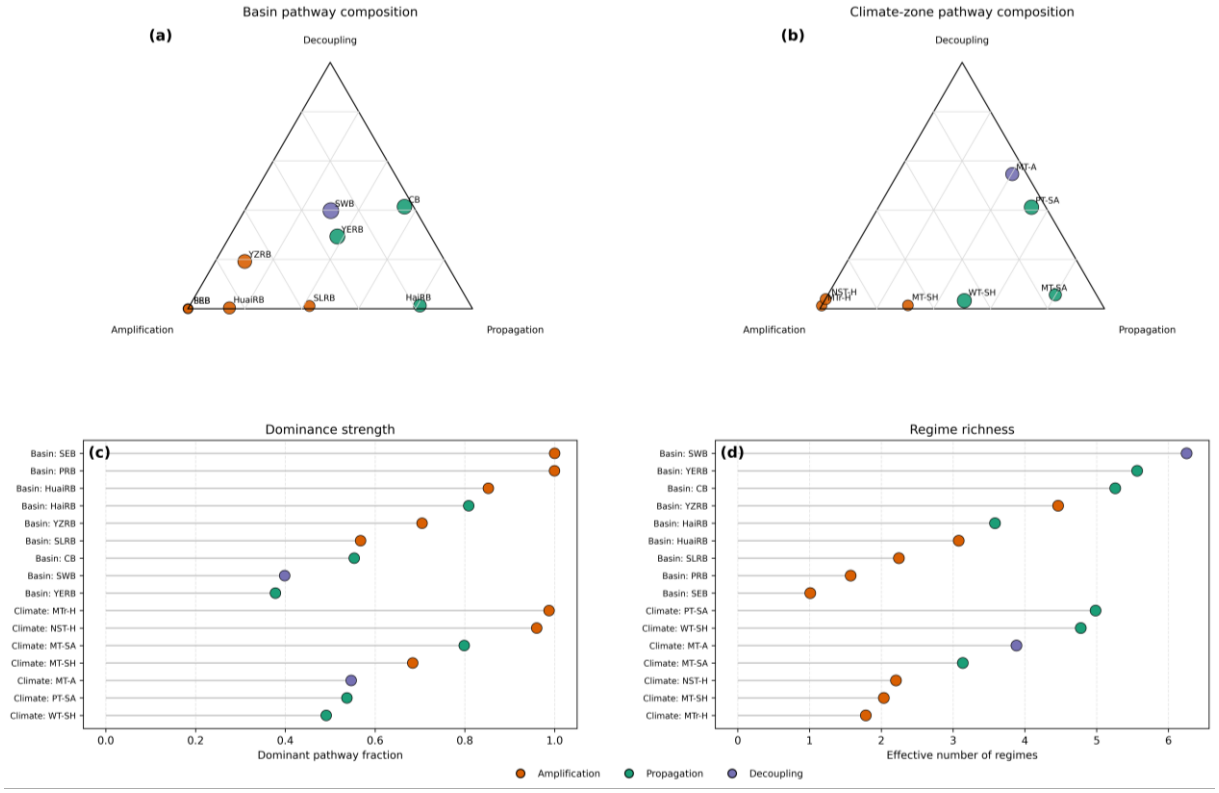

Figure 7. Regional pathway attribution of hydrological response regimes. Panels (a) and (b) show basin and climate-zone pathway compositions in ternary space. Panel (c) compares dominant pathway fractions across regions. Panel (d) shows regime richness, indicating the degree of regional response heterogeneity.

https://doi.org/10.5194/egusphere-2026-2963
Preprint. Discussion started: 23 June 2026

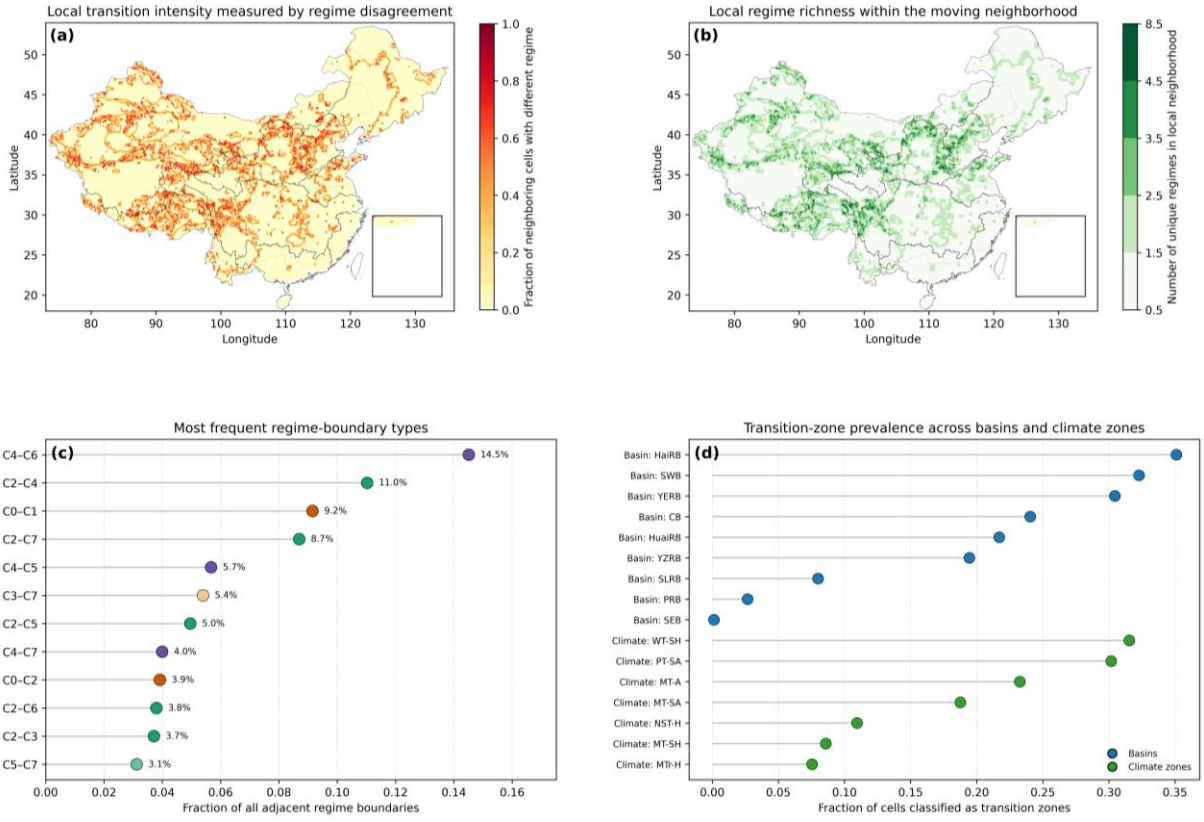

Figure 8. Spatial transition belts and mixing hotspots of the response-regime framework. Panel (a) maps local transition intensity based on neighborhood regime disagreement. Panel (b) shows local regime richness. Panel (c) identifies the most frequent regime-boundary types. Panel (d) summarizes transition-zone prevalence across basins and climate zones.

4.4 Coupling between compound-event types and hydrological response regimes

The relationship between compound-event types and response regimes showed that the eight regimes were not equivalent to the four event types (Figure 9). Instead, each regime represented a distinct way in which multiple event types were organized and transformed into hydrological responses. Across most regimes, warm-dry and cold-wet events contributed the largest fractions, but their conditional intensity and enrichment patterns differed substantially among regimes.

The event-to-regime coupling diagram showed that warm-dry and cold-wet events were distributed across multiple response regimes. This indicates that the same event type can produce different response behaviors depending on antecedent conditions, propagation pathways, seasonality, and regional hydroclimatic setting. For example, C0 and C1 were associated with stronger positive conditional intensity under warm-dry and cold-wet conditions, supporting their interpretation as amplified and seasonal high-intensity regimes. In contrast, C4, C5, and C6 showed weaker or negative conditional intensity, indicating that these regimes are not defined by event occurrence alone but by weaker hydrological amplification, persistence, or transition-dominated behavior.

https://doi.org/10.5194/egusphere-2026-2963
Preprint. Discussion started: 23 June 2026

The event-regime enrichment analysis further distinguished regimes with specific event-type preferences. C6 showed strong enrichment of cold-dry and warm-wet events, consistent with its mixed-transition interpretation. C1 and C3 also exhibited positive enrichment for selected event types, whereas C5 and C7 showed depletion in some event categories despite their strong memory or propagation signatures. This confirms that response regimes cannot be reduced to simple event categories. Instead, they represent combinations of event composition, conditional severity, hydrological transformation, and antecedent-state dependence.

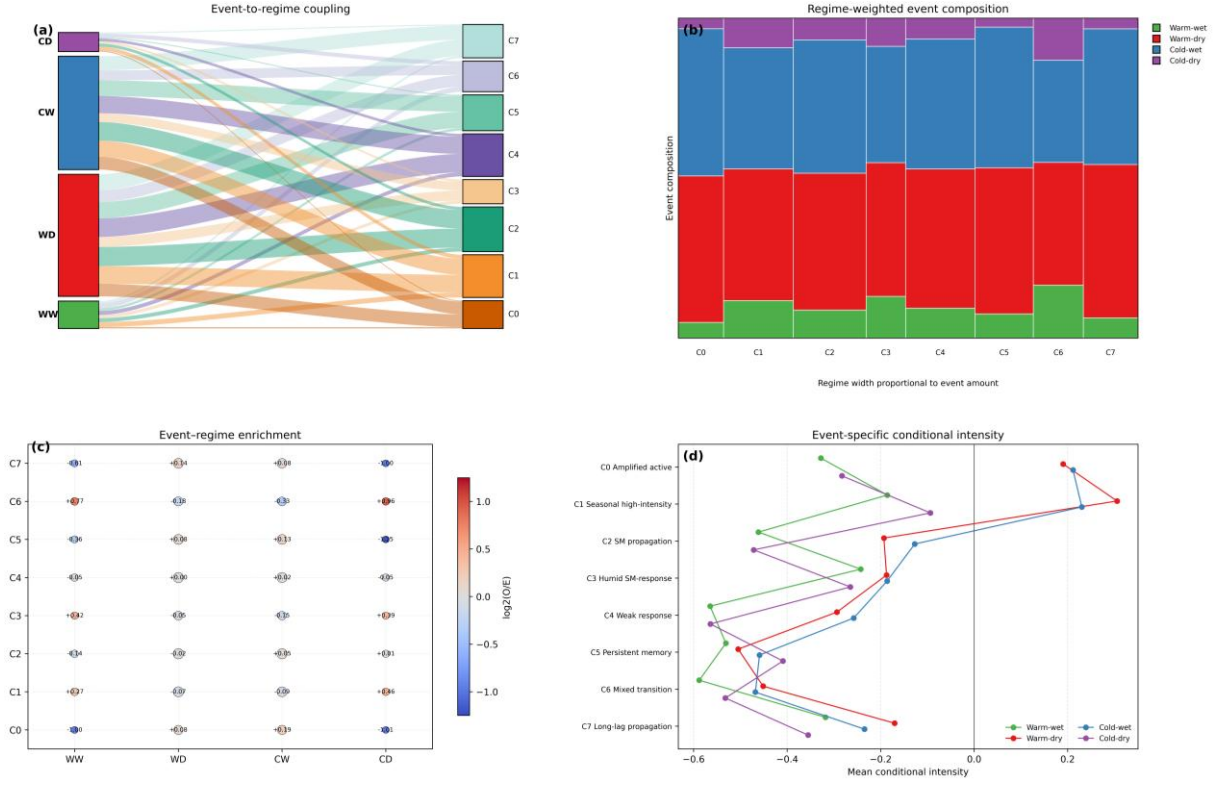

Figure 9. Coupling between compound-event types and hydrological response regimes. Panel (a) shows the coupling between four compound-event types and eight response regimes. Panel (b) presents regime-weighted event composition. Panel (c) shows event-regime enrichment. Panel (d) compares event-specific conditional intensity across regimes.

Thus, the regime framework provides an event-conditioned but response-centered classification, bridging the gap between compound-event occurrence and hydrological-system behavior.

4.5 Antecedent-memory sensitivity and pathway-level synthesis

Antecedent-memory effects varied strongly among the eight response regimes (Figure 10). C0 and C1 maintained positive conditional intensity across different memory windows, indicating that amplification regimes remained sensitive to antecedent hydroclimatic states while preserving strong event response. In contrast, C4, C5, and C6 generally showed negative conditional intensity, suggesting weaker or more delayed hydrological responses. The memory-sensitivity ranking showed that C4, C0,

https://doi.org/10.5194/egusphere-2026-2963
Preprint. Discussion started: 23 June 2026

C1, and C5 were among the most sensitive regimes to the extension of antecedent windows, whereas C2 and C3 were less sensitive to the tested memory-window changes.

C5 displayed a distinct memory-adjustment behavior, particularly under selected event types. This supports its interpretation as a persistent-memory regime, in which long-duration event behavior and same-type transition probability are more important than instantaneous event intensity. C7 showed a more moderate but consistent long-lag propagation signal, indicating that its defining feature is not necessarily strong immediate intensity but delayed transfer from meteorological moisture anomalies to soil moisture and runoff.

The pathway synthesis summarized the eight regimes into three hydrological response pathways (Figure 11). The amplification pathway, consisting of C0, C1, and C3, was characterized by stronger severity and seasonality-related signals. The propagation pathway, consisting of C2, C5, and C7, showed stronger persistence, antecedent-state, and propagation-related behavior, indicating that soil-moisture storage and runoff response mediate compound-event impacts. The decoupling pathway, consisting of C4 and C6, was associated with weaker hydrological amplification but stronger transition or boundary behavior.

This pathway-level synthesis indicates that China's compound hydroclimatic responses are organized by multiple hydrological mechanisms rather than by a single national gradient of event frequency, severity, or aridity.

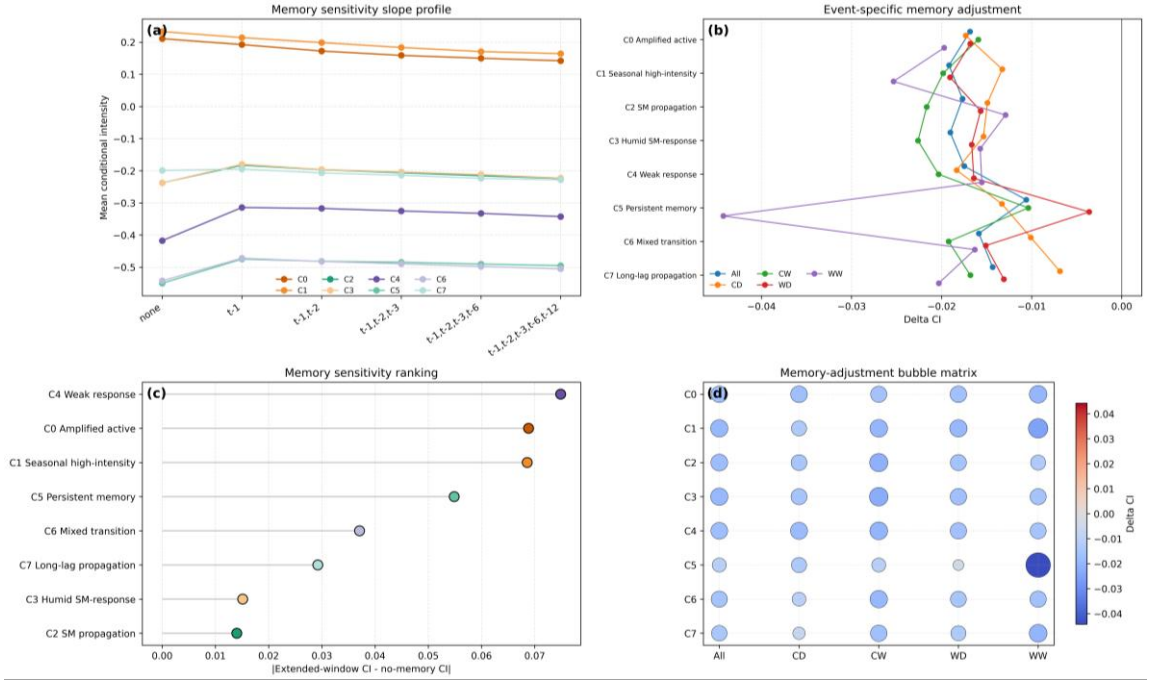

Figure 10. Regime-conditioned antecedent-memory response. Panel (a) shows conditional intensity under different antecedent-memory windows. Panel (b) presents event-specific memory adjustment by regime. Panel (c) ranks regimes according to memory sensitivity. Panel (d) summarizes memory-adjustment patterns using a bubble matrix.

https://doi.org/10.5194/egusphere-2026-2963
Preprint. Discussion started: 23 June 2026

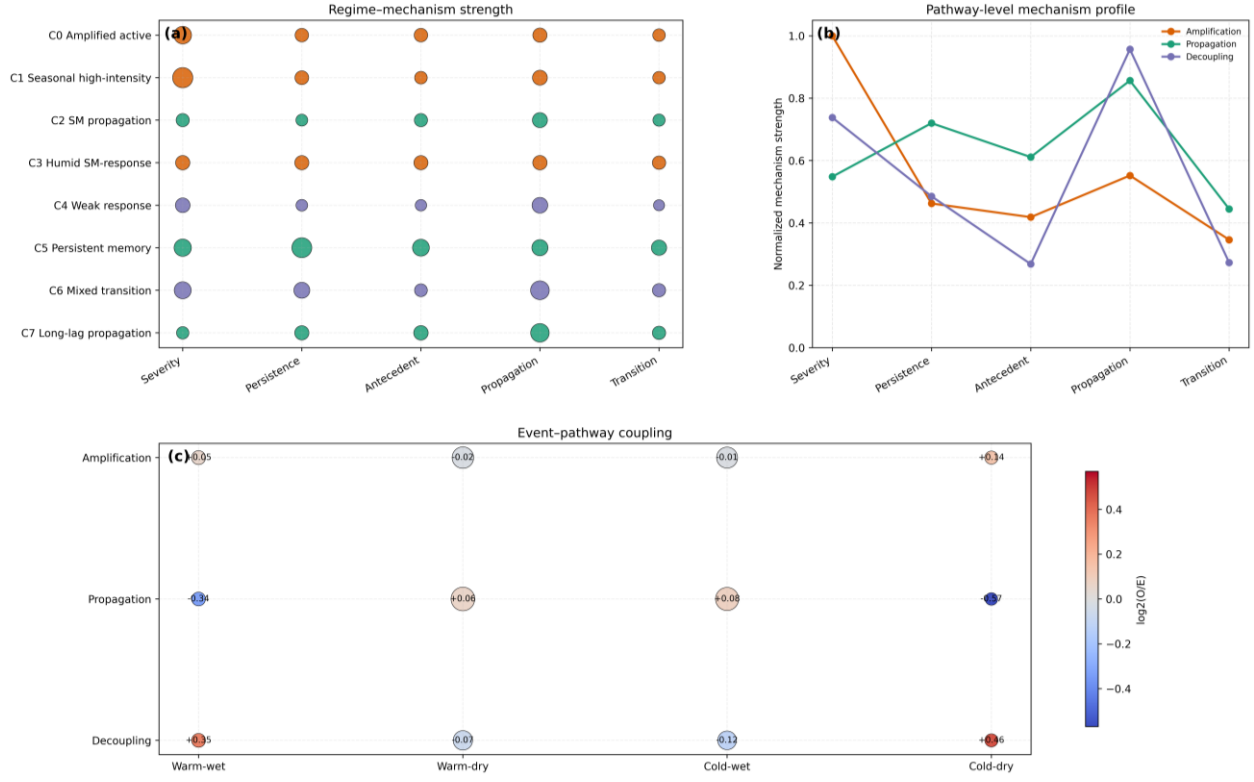

Figure 11. Data-driven synthesis of hydrological response pathways. Panel (a) compares regime-level mechanism strength. Panel (b) summarizes pathway-level mechanism profiles. Panel (c) shows event-pathway coupling, highlighting how compound-event types are organized through amplification, propagation-memory, and weak-transition pathways.

5 Discussion

5.1 Moving from event-type mapping to response-regime diagnosis

A key implication of this study is that compound hydroclimatic events should not be interpreted only through event-type categories. Warm-wet, warm-dry, cold-wet, and cold-dry events provide a useful first-order classification of hydroclimatic anomalies, but they do not fully determine hydrological response. The same event type may be associated with amplified response, weak response, persistent memory, or long-lag propagation depending on regional storage, antecedent state, seasonal timing, and soil-moisture–runoff coupling. This interpretation is consistent with recent evidence that drought-induced hydrological responses differ substantially among climate regimes and that precipitation deficits can propagate through soil moisture, runoff, and evapotranspiration with different response rates and recovery behaviors (Liu et al., 2024b). It is also supported by recent drought-propagation studies showing that meteorological, agricultural, and hydrological droughts are interconnected but that their propagation probability and dynamics vary with watershed storage, baseflow conditions, climatic aridity, and regional controls (Yan et al., 2025).

https://doi.org/10.5194/egusphere-2026-2963
Preprint. Discussion started: 23 June 2026

The proposed response-regime framework shifts the focus from event occurrence to event transformation within the hydrological system. This shift is important because hydroclimatic risk is not determined only by whether a compound event occurs, but also by how the system stores, propagates, amplifies, or dampens the anomaly. Recent work on consecutive hydrological extremes further indicates that drought-to-flood transitions cannot be adequately characterized by treating droughts and floods as independent events, because transition detection and interpretation depend strongly on timing, threshold choice, seasonality, and catchment context (Anderson et al., 2025). Therefore, the behavior-feature regionalization developed in this study provides a response-based diagnostic tool that integrates multiple hydrological dimensions into interpretable regimes, including event occurrence, persistence, antecedent memory, propagation, and transition behavior.

This approach is particularly useful for large heterogeneous regions such as China. Conventional basin or climate-zone classifications cannot fully represent the diversity of compound-event responses within each region. Recent catchment-classification work in mainland China has shown that hydrological behavior varies strongly among basin clusters and is controlled not only by climate but also by soil and catchment characteristics (Xu et al., 2024). The results of this study further show that major basins often contain multiple response regimes and that transition belts can occur within or across conventional regional boundaries. Thus, response-regime regionalization offers a complementary way to interpret hydroclimatic risk beyond static geographic divisions.

5.2 Mechanistic meaning of amplification, propagation-memory, and decoupling pathways

The three response pathways summarize different hydrological mechanisms. The amplification pathway represents regions where compound events are more likely to translate into strong conditional hydrological responses. These areas are mainly associated with humid and monsoonal settings, where seasonal water-energy interactions can rapidly amplify event impacts. The seasonal high-intensity regime within this pathway suggests that the timing of compound events is central to their hydrological impact (Liu et al., 2024b; Xu et al., 2024).

The propagation pathway reflects the delayed transfer of meteorological anomalies through soil moisture and runoff. This pathway is especially relevant for semiarid, transitional, and storage-controlled environments, where antecedent moisture conditions regulate the persistence and timing of hydrological anomalies. The soil-moisture propagation and long-lag propagation regimes indicate that hydrological risk may emerge not only during the event month but also through lagged land-surface and runoff responses (Anderson et al., 2025; Li et al., 2026).

The decoupling pathway represents regions where event occurrence does not necessarily lead to strong hydrological amplification. This may occur because of weak soil-moisture–runoff coupling, arid background conditions, mixed event transitions, or complex local controls. Recent evidence also suggests that drought conditions can reduce streamflow sensitivity to precipitation, particularly in arid regions, indicating that hydroclimatic anomalies do not always propagate into proportional runoff responses. Importantly, weak-response regions should not be interpreted as risk-free. Their high transition intensity and boundary behavior suggest that changes in antecedent state, event sequence, or seasonal timing may shift these regions toward stronger response modes (Li et al., 2025; Matanó et al., 2025).

https://doi.org/10.5194/egusphere-2026-2963
Preprint. Discussion started: 23 June 2026

The similarity hierarchy and spatial transition analysis further suggest that response pathways are not sharply separated in space. Instead, they form a continuum of regime cores and transition belts. This is especially important for interpreting hydrological risk in boundary regions, where small changes in antecedent conditions or seasonal timing may shift the system from one response pathway to another. This interpretation is consistent with catchment-classification studies showing that hydrological behavior varies continuously across hydroclimatic and soil-control gradients rather than following purely static administrative, basin, or climate-zone boundaries.

5.3 Implications for regional hydroclimatic risk assessment

The basin-scale results show that major river basins cannot be treated as internally uniform response units. Basins with high regime richness or high transition-zone prevalence contain multiple response pathways and therefore require differentiated monitoring strategies. In amplification-dominated basins, monitoring should prioritize seasonal compound-event intensity and rapid hydrological response. In propagation-dominated regions, antecedent soil moisture, runoff memory, and lagged meteorological deficits should be emphasized, as drought propagation studies have shown that meteorological anomalies can evolve into agricultural or hydrological droughts through delayed land-surface responses (Muthuvel and Qin, 2025; Ning et al., 2025). In decoupling regions, monitoring should focus on boundary conditions under which otherwise weak responses may shift into stronger hydrological anomalies, especially in areas affected by abrupt wet–dry transitions (Liang et al., 2025).

This regime-based perspective can support more targeted hydroclimatic risk assessment. Instead of applying a single national event threshold or one basin-scale response model, hydrological monitoring and early warning can be adapted to the dominant response pathway and local transition intensity. Regions with high transition intensity require particular attention because they represent spatially mixed and potentially more uncertain response mechanisms.

The results also have implications for model evaluation. Hydrological models or climate-impact assessments should not only reproduce event frequency and intensity but also capture the correct response regime(Chen et al., 2025). A model may simulate warm-dry or cold-wet event occurrence reasonably well, yet still fail to represent soil-moisture memory, runoff propagation, or transition behavior. The proposed regime framework therefore provides a diagnostic basis for evaluating whether models reproduce the mechanisms that organize compound-event impacts (Heuer et al., 2025).

5.4 Limitations and future perspectives

Several limitations remain. First, the response regimes are derived from gridded standardized indices, and their interpretation depends on the quality and consistency of the underlying temperature, moisture, soil-moisture, and runoff datasets. Uncertainty in any of these inputs may influence the derived behavior features and cluster assignments. Second, the clustering framework is designed to identify dominant long-term behavior and does not explicitly resolve individual event causality or localized hydrological processes. Third, the analysis focuses on historical behavior, while future changes in compound-event response regimes under climate change remain to be examined. Fourth, some spatial transition regions show mixed behavior, suggesting that fuzzy or probabilistic regime classification may be useful in future work.

https://doi.org/10.5194/egusphere-2026-2963
Preprint. Discussion started: 23 June 2026

Future research should extend this response-regime framework to future climate projections, event-based hydrological modeling, and basin-specific early-warning systems. It would also be useful to test whether the identified response pathways remain stable under changing hydroclimatic conditions and whether regime transitions can serve as early indicators of shifts in hydrological risk.

6 Conclusions

This study developed a behavior-space regionalization framework to diagnose hydrological response regimes of compound hydroclimatic events across China. By integrating event occurrence, conditional severity, persistence, seasonality, antecedent state, propagation coupling, transition behavior, and threshold sensitivity, the framework moves beyond conventional event-type mapping and provides a response-centered interpretation of compound hydroclimatic risk.

Eight hydrological response regimes were identified: amplified active, seasonal high-intensity, soil-moisture propagation, humid soil-moisture response, weak response, persistent memory, mixed transition, and long-lag propagation. These regimes are not arbitrary clusters. They show distinct behavior fingerprints, hierarchical similarity structure, event-type coupling, antecedent-memory sensitivity, and spatial organization.

The eight regimes can be further organized into three response pathways: amplification, propagation, and decoupling. Amplification regimes dominate parts of southern and humid China, propagation regimes are prominent in northern, transitional, and storage-controlled regions, while decoupling regimes appear in arid, complex, or boundary regions. Spatial transition analysis further reveals that regime mixing is concentrated along hydroclimatic transition belts and basin-climate boundaries.

These findings indicate that compound hydroclimatic risk across China is organized by multiple hydrological response pathways rather than by a single gradient of event frequency or intensity. The proposed response-regime framework provides a basis for region-specific monitoring, hydrological attribution, and future assessment of compound-event impacts.

Code and data availability

This study used five gridded monthly datasets over China, including precipitation from CHM PRE V2(Hu et al., 2025), potential evaporation from GLEAM V4.2(Miralles et al., 2025), mean temperature from CMFD V2(He et al., 2025), runoff from CNRD v1.0(Gou et al., 2021), and soil moisture from fusing ERA5-land and SMAP L4(Wang et al., 2026), to derive the SPEI, STI, SRI, and SSMI indices used in the analysis. The code used for dynamic event identification, lag-aware conditional intensity estimation, clustering, and regional attribution analysis is publicly available at GitHub (https://github.com/theshyyi/Earth-s-Future-code). The main data are publicly archived in Zenodo and are available at https://doi.org/10.5281/zenodo.19682148.

https://doi.org/10.5194/egusphere-2026-2963
Preprint. Discussion started: 23 June 2026

Author contributions

LE Xinlong: Writing – review & editing, Writing – original draft, Visualization, Validation, Software, Methodology, Investigation, Formal analysis, Data curation, Conceptualization, Software. KANG Ling: Project administration, Funding acquisition. ZHOU Liwei: Supervision, Software, Methodology.

Competing interests

The authors declare that they have no known competing financial interests or personal relationships that could have appeared to influence the work reported in this paper.

Disclaimer

The authors declare there are no conflicts of interest for this manuscript.

Acknowledgements

The computation is completed in the HPC Platform of Huazhong University of Science and Technology. The authors declare that they have no financial conflicts of interest or other competing interests relevant to this study.

Financial support

This work was supported the National Key R&D Program of China (Grant No. 2023YFC3209204), the Hubei Water Conservancy Research Program (HBSLKY202412), and the Fundamental Research Funds for the Central Universities, HUST (2025JYCXJJ056).

Review statement

The review statement will be added by Copernicus Publications listing the handling editor as well as all contributing referees according to their status anonymous or identified.

References

Aihaiti, A., Jiang, Z., Zhu, L., Li, W., and You, Q.: Risk changes of compound temperature and precipitation extremes in China under 1.5 °C and 2 °C global warming, Atmos. Res., 264, https://doi.org/10.1016/j.atmosres.2021.105838, 2021.

https://doi.org/10.5194/egusphere-2026-2963
Preprint. Discussion started: 23 June 2026

Anderson, B. J., Muñoz-Castro, E., Tallaksen, L. M., Matano, A., Götte, J., Armitage, R., Magee, E., and Brunner, M. I.: What is a drought-to-flood transition? Pitfalls and recommendations for defining consecutive hydrological extreme events, Hydrol. Earth Syst. Sci., 29, 6069–6092, https://doi.org/10.5194/hess-29-6069-2025, 2025.

Chen, Y., Zhang, N., Zhang, X., Wang, G., Wang, Y., Liu, R., and Ma, M.: A novel dynamic flash flood early warning framework based on distributed hydrologic modeling, Ecological Indicators, 172, 113247, https://doi.org/10.1016/j.ecolind.2025.113247, 2025.

Gou, J., Miao, C., Samaniego, L., Xiao, M., Wu, J., and Guo, X.: CNRD v1.0: A high-quality natural runoff dataset for hydrological and climate studies in China, Bull. Am. Meteorol. Soc., 102, E929–E947, https://doi.org/10.1175/BAMS-D-20-0094.1, 2021.

Gupta, A. and Karthikeyan, L.: Role of initial conditions and meteorological drought in soil moisture drought propagation: An event-based causal analysis over south asia, Earth's Future, 12, e2024EF004674, https://doi.org/10.1029/2024EF004674, 2024.

Hao, Z., Singh, V., and Hao, F.: Compound extremes in hydroclimatology: a review, Water, 10, https://doi.org/10.3390/w10060718, 2018.

Hao, Z., Hao, F., Xia, Y., Feng, S., Sun, C., Zhang, X., Fu, Y., Hao, Y., Zhang, Y., and Meng, Y.: Compound droughts and hot extremes: Characteristics, drivers, changes, and impacts, Earth Sci. Rev., 235, 104241, https://doi.org/10.1016/j.earscirev.2022.104241, 2022.

He, J., Yang, K., Li, X., Tang, W., Shao, C., Jiang, Y., and Ding, B.: China meteorological forcing dataset v2.0 (1951-2024), https://doi.org/10.11888/Atmos.tpdc.302088, 2025.

Heuer, M. M., Mohajerani, H., and Casper, M. C.: Finding process-behavioural parameterisations of a hydrological model using a multi-step process-based calibration and evaluation scheme, Hydrol. Earth Syst. Sci., 29, 3503–3525, https://doi.org/10.5194/hess-29-3503-2025, 2025.

Hu, J., Miao, C., Su, J., Zhang, Q., Gou, J., and Sun, Q.: A new upgraded high-precision gridded precipitation dataset considering spatiotemporal and physical correlations for mainland China, Earth Syst. Sci. Data Discuss., 1–27, https://doi.org/10.5194/essd-2025-20, 2025.

Leonard, M., Westra, S., Phatak, A., Lambert, M., van den Hurk, B., McInnes, K., Risbey, J., Schuster, S., Jakob, D., and Stafford-Smith, M.: A compound event framework for understanding extreme impacts, WIREs Clim. Change, 5, 113–128, https://doi.org/10.1002/wcc.252, 2014.

Li, X., Cui, P., Shen, P., and Zhang, X.: Unraveling scale-dependent flood responses to changing climate extremes over the tibetan plateau, Commun. Earth Environ., 7, 252, https://doi.org/10.1038/s43247-026-03413-2, 2026.

Li, Y., Huang, Y., Li, Y., Zhang, H., Fan, J., Deng, Q., and Wang, X.: Spatiotemporal heterogeneity in meteorological and hydrological drought patterns and propagations influenced by climatic variability, LULC change, and human regulations, Sci. Rep., 14, 5965, https://doi.org/10.1038/s41598-024-56526-z, 2024.

Li, Y., Deng, Q., Chang, J., Huang, Y., Zhang, H., Fan, J., and Wu, H.: Nonlinear propagation of meteorological to hydrological drought: Contrasting dynamics in humid and semi-arid regions, J. Hydrol., 657, 133012, https://doi.org/10.1016/j.jhydrol.2025.133012, 2025.

https://doi.org/10.5194/egusphere-2026-2963
Preprint. Discussion started: 23 June 2026

Liang, Y., Han, P., Kim, T.-W., Zhang, X., Li, Z., Liu, H., and Chen, S.: Development of drought-flood abrupt alternations identification method based on daily soil moisture index: Spatiotemporal characterization and risk assessment in the middle and lower reaches of yangtze river basin, J. Hydrol.: Reg. Stud., 61, 102690, https://doi.org/10.1016/j.ejrh.2025.102690, 2025.

Liu, H., Xiao, P., Zhang, X., Liang, Y., Tang, B., Chen, S., and Liu, Y.: Winter snowpack loss increases warm-season compound hot-dry extremes, Commun. Earth Environ., 5, 567, https://doi.org/10.1038/s43247-024-01734-8, 2024a.

Liu, Q., Liang, L., Sun, T., Wang, X., Yan, D., and Li, C.: Hydrological response of drought impacts across catchments worldwide, Sci. Total Environ., 931, 172912, https://doi.org/10.1016/j.scitotenv.2024.172912, 2024b.

Liu, Y., Hu, T., Yang, J., and Yu, L.: Understanding meteorological, runoff, and agricultural drought propagation and their influencing factors in an ensemble of multiple datasets, Hydrol. Earth Syst. Sci., 30, 2775–2795, https://doi.org/10.5194/hess-30-2775-2026, 2026.

Ma, Q., Ni, B., Li, Z., Sun, J., Zhang, Q., Qi, P., Wu, Y., Zhang, G., and Li, H.: Propagation of different types of compound drought-hot events: Spatiotemporal patterns and response relationship, J. Hydrol.: Reg. Stud., 63, 103031, https://doi.org/10.1016/j.ejrh.2025.103031, 2026.

Manning, C., Widmann, M., Bevacqua, E., Van Loon, A., Maraun, D., and Vrac, M.: Soil moisture drought in Europe: a compound event of precipitation and potential evapotranspiration on multiple time scales, J. Hydrometeorol., 19, 1255–1271, https://doi.org/10.1175/JHM-D-18-0017.1, 2018.

Massari, C., Pellet, V., Tramblay, Y., Crow, W. T., Gründemann, G. J., Hascoetf, T., Penna, D., Modanesi, S., Brocca, L., Camici, S., and Marra, F.: On the relation between antecedent basin conditions and runoff coefficient for European floods, J. Hydrol., 625, 130012, https://doi.org/10.1016/j.jhydrol.2023.130012, 2023.

Matanó, A., Hamed, R., Brunner, M. I., Barendrecht, M. H., and Van Loon, A. F.: Drought decreases annual streamflow response to precipitation, especially in arid regions, Hydrol. Earth Syst. Sci., 29, 2749–2764, https://doi.org/10.5194/hess-29-2749-2025, 2025.

Miralles, D. G., Bonte, O., Koppa, A., Baez-Villanueva, O. M., Tronquo, E., Zhong, F., Beck, H. E., Hulsman, P., Dorigo, W., Verhoest, N. E. C., and Haghdoost, S.: GLEAM4: Global land evaporation and soil moisture dataset at 0.1° resolution from 1980 to near present, Sci. Data, 12, 416, https://doi.org/10.1038/s41597-025-04610-y, 2025.

Muthuvel, D. and Qin, X.: Probabilistic analysis of future drought propagation, persistence, and spatial concurrence in monsoon-dominant asian regions under climate change, Hydrol. Earth Syst. Sci., 29, 3203–3225, https://doi.org/10.5194/hess-29-3203-2025, 2025.

Ning, S., Zhang, M., Xu, X., Zhou, Y., Jin, J., Xu, L., Udmale, P., and Thapa, B. R.: Spatiotemporal propagation of compound drought events in China: An approach combining 3D clustering and daily-scale extended convergent cross mapping, J. Hydrol., https://doi.org/10.2139/ssrn.5127582, 2025.

Niu, J., Zhang, K., Li, X., and Bao, H.: Integrated catchment classification across China based on hydroclimatological and geomorphological similarities using self-organizing map and fuzzy *c*-means clustering for hydrological modeling, Hydrol. Earth Syst. Sci., 30, 2013–2036, https://doi.org/10.5194/hess-30-2013-2026, 2026.

Pan, X., Wang, W., Shao, Q., Wei, J., Li, H., Zhang, F., Cao, M., and Yang, L.: Compound drought and heat waves variation and association with SST modes across china, Sci. Total Environ., 907, https://doi.org/10.1016/j.scitotenv.2023.167934, 2024.

https://doi.org/10.5194/egusphere-2026-2963
Preprint. Discussion started: 23 June 2026

Seneviratne, S. I., Corti, T., Davin, E. L., Hirschi, M., Jaeger, E. B., Lehner, I., Orlowsky, B., and Teuling, A. J.: Investigating soil moisture–climate interactions in a changing climate: A review, Earth-Science Reviews, 99, 125–161, https://doi.org/10.1016/j.earscirev.2010.02.004, 2010.

Shukla, S. and Wood, A. W.: Use of a standardized runoff index for characterizing hydrologic drought, Geophys. Res. Lett., 35, https://doi.org/10.1029/2007GL032487, 2008.

Sutanto, S. J., Duku, C., Gülveren, M., Dankers, R., and Paparrizos, S.: Future intensification of compound and consecutive drought and heatwave risks in europe, Nat. Hazards Earth Syst. Sci., 25, 3879–3895, https://doi.org/10.5194/nhess-25-3879-2025, 2025.

Tripathy, K. P., Mukherjee, S., Mishra, A. K., Mann, M. E., and Williams, A. P.: Climate change will accelerate the high-end risk of compound drought and heatwave events, Proc. Natl. Acad. Sci. U.S.A., 120, e2219825120, https://doi.org/10.1073/pnas.2219825120, 2023.

Van Loon, A. F.: Hydrological drought explained, WIREs Water, 2, 359–392, https://doi.org/10.1002/wat2.1085, 2015.

Van Loon, A. F., Kchouk, S., Matanó, A., Tootoonchi, F., Alvarez-Garreton, C., Hassaballah, K. E. A., Wu, M., Wens, M. L. K., Shyrokaya, A., Ridolfi, E., Biella, R., Nagavciuc, V., Barendrecht, M. H., Bastos, A., Cavalcante, L., de Vries, F. T., Garcia, M., Mård, J., Streefkerk, I. N., Teutschbein, C., Tootoonchi, R., Weesie, R., Aich, V., Boisier, J. P., Di Baldassarre, G., Du, Y., Galleguillos, M., Garreaud, R., Ionita, M., Khatami, S., Koehler, J. K. L., Luce, C. H., Maskey, S., Mendoza, H. D., Mwangi, M. N., Pechlivanidis, I. G., Ribeiro Neto, G. G., Roy, T., Stefanski, R., Trambauer, P., Koebele, E. A., Vico, G., and Werner, M.: Review article: Drought as a continuum – memory effects in interlinked hydrological, ecological, and social systems, Nat. Hazards Earth Syst. Sci., 24, 3173–3205, https://doi.org/10.5194/nhess-24-3173-2024, 2024.

Vicente-Serrano, S. M., Beguería, S., and López-Moreno, J. I.: A multiscalar drought index sensitive to global warming: The standardized precipitation evapotranspiration index, J. Clim., 23, 1696–1718, https://doi.org/10.1175/2009JCLI2909.1, 2010.

Wang, A., Tao, H., Ding, G., Zhang, B., Huang, J., and Wu, Q.: Global cropland exposure to extreme compound drought heatwave events under future climate change, Weather Clim. Extremes, 40, 100559, https://doi.org/10.1016/j.wace.2023.100559, 2023.

Wang, W., Feng, S., Zhang, Y., Wei, Z., Dong, J., Weihermüller, L., Liu, C.-Q., and Vereecken, H.: Fusing ERA5-land and SMAP L4 for an improved global soil moisture product (1950–2025), Earth Syst. Sci. Data, 18, 1061–1088, https://doi.org/10.5194/essd-18-1061-2026, 2026.

Wang, X., Tu, X., Peng, T., Singh, V. P., Zhou, Z., and Lin, K.: Analysis of drought propagation from meteorological to hydrological drought under the impact of a super-large reservoir, J. Hydrol.: Reg. Stud., 62, 102801, https://doi.org/10.1016/j.ejrh.2025.102801, 2025.

Xu, H., Wang, H., and Liu, P.: Identifying control factors of hydrological behavior through catchment classification in mainland of China, J. Hydrol., 645, 132206, https://doi.org/10.1016/j.jhydrol.2024.132206, 2024.

Yan, H., Sun, N., Yao, L., Thurber, T. B., and Rice, J. S.: Rising temperatures intensify drought propagation and severity across the contiguous united states, npj Nat. Hazards, 2, 91, https://doi.org/10.1038/s44304-025-00134-y, 2025.

Yang, X., Xie, L., Luo, D., and Ye, Z.: Evaluating the propagation characteristics of meteorological drought to hydrological drought using a three-dimensional method, J. Hydrol., 662, 133930, https://doi.org/10.1016/j.jhydrol.2025.133930, 2025.

https://doi.org/10.5194/egusphere-2026-2963
Preprint. Discussion started: 23 June 2026

Ye, L., Shi, K., Xin, Z., Wang, C., and Zhang, C.: Compound droughts and heat waves in China, Sustainability, 11, https://doi.org/10.3390/su11123270, 2019.

You, Z., Sun, X., Sun, H., Chen, L., Lu, M., Xue, J., Ban, X., Yan, B., Tuo, Y., Qin, H., Zhang, L., and Zhang, W.: Mechanisms of meteorological drought propagation to agricultural drought in China: Insights from causality chain, Npj Nat. Hazards, 2, 1–15, https://doi.org/10.1038/s44304-025-00073-8, 2025.

Zhang, W., Luo, M., Gao, S., Chen, W., Hari, V., and Khouakhi, A.: Compound hydrometeorological extremes: drivers, mechanisms and methods, Front. Earth Sci., 9, https://doi.org/10.3389/feart.2021.673495, 2021.

Zscheischler, J., Westra, S., van den Hurk, B., Seneviratne, S., Ward, P., Pitman, A., AghaKouchak, A., Bresch, D., Leonard, M., Wahl, T., and Zhang, X.: Future climate risk from compound events, Nat. Clim. Change, 8, 469–477, https://doi.org/10.1038/s41558-018-0156-3, 2018.

Zscheischler, J., Martius, O., Westra, S., Bevacqua, E., Raymond, C., Horton, R. M., van den Hurk, B., AghaKouchak, A., Jézéquel, A., Mahecha, M. D., Maraun, D., Ramos, A. M., Ridder, N. N., Thiery, W., and Vignotto, E.: A typology of compound weather and climate events, Nat Rev Earth Environ, 1, 333–347, https://doi.org/10.1038/s43017-020-0060-z, 2020.

Buiter, S.: How syn-rift sedimentation promotes the formation of hyper-extended margins, EGU General Assembly 2020, Online, 4–8 May 2020, EGU2020-18622, https://doi.org/10.5194/egusphere-egu2020-18622, 2020.

Loew, A., Bennartz, R., Fell, F., Lattanzio, A., Doutriaux-Boucher, M., and Schulz, J.: Surface Albedo Validation Sites, EUMETSAT [data set], https://doi.org/10.15770/EUM_SEC_CLM_1001, 2015.

Porter, J. G., De Bruyn, W., and Saltzman, E. S.: Eddy flux measurements of sulfur dioxide deposition to the sea surface, Atmos. Chem. Phys., 18, 15291–15305, https://doi.org/10.5194/acp-18-15291-2018, 2018.

Jung, M., Koirala, S., Weber, U., Ichii, K., Gans, F., Gustau-Camps-Valls, Papale, D., Schwalm, C., Tramontana, G., and Reichstein, M.: The FLUXCOM ensemble of global land-atmosphere energy fluxes, arXiv [preprint], arXiv:1812.04951, 11 December 2018.

Randall, D., Dazlich, D., Heikes, R., and Konor, C.: CSU model for DCMIP 2016, Zenodo [code], https://doi.org/10.5281/zenodo.5800992018, 2017.

Singh, O. N. and Fabian, P. (Eds.): Atmospheric Ozone: a Millennium Issue, Copernicus Publications, Katlenburg-Lindau, Germany, 147 pp., ISBN 393658608X, 2003.

van Edig, X., Schwarze, S., and Zeller, M.: The robustness of indicator based poverty assessment tools in changing environments – empirical evidence from Indonesia, in: Tropical Rainforests and Agroforests under Global Change, Environmental Science and Engineering (Environmental Engineering), edited by: Tscharntke, T., Leuschner, C., Veldkamp, E., Faust, H., Guhardja, E., and Bidin, A., Springer, Berlin, Heidelberg, Germany, 191–211, https://doi.org/10.1007/978-3-642-00493-3_9, 2010.